ELSEVIER

International Journal of Mass Spectrometry 210/211 (2001) 387–402

www.elsevier.com/locate/ijms

Influence of fluorine substitution on the structures and thermochemistry of chloride ion–ether complexes in the gas phase

B. Bogdanov, H.J.S. Lee, T.B. McMahon

Department of Chemistry, University of Waterloo, Waterloo, Ontario N2L 3G1, Canada

Abstract

The thermochemistry of the chloride ion clustering onto dimethyl ether, diethyl ether, and three fluorinated ethers (CH_3OCF_3, $(CF_2H)_2O$, and CF_3OCF_2H) under thermal equilibrium conditions has been determined using pulsed-ionization high pressure mass spectrometry. The standard enthalpy ($\Delta H°$) and entropy change ($\Delta S°$) values obtained indicate a variety of different types of bonding in these complexes. The mode of binding is mainly determined by the number of fluorine atoms present and by the substitution pattern. In addition ab initio computational methods have been used to obtain more insight into the structures and energetics. $\Delta H°_{298}$ value calculated at the MP2/[6-311 ++ G(3*df*,3*pd*)/6-311 + G(2*df*,*p*)]//MP2/[6-31 + G(*d*)/6-31G(*d*)] level of theory show excellent agreement with the experimentally obtained $\Delta H°$ values. (Int J Mass Spectrom 210/211 (2001) 387–402) © 2001 Elsevier Science B.V.

Keywords: Chloride ion–(fluorinated) ether complexes; Structures; Thermochemistry; PHPMS; Ab initio computations

1. Introduction

The study of structures and thermochemistry of solvated gas phase ions continues to be an active field of research, providing insight into solvation processes, and the difference in intrinsic reactivity between the gas and condensed phases [1–5]. Especially interesting are systems where multiple binding interactions are possible. In both the gas [6–11] and condensed phases, metal ion–crown ether complexes have been studied extensively, both experimentally and theoretically [12]. Less attention has been paid to weakly bound anion containing complexes, where multiple binding interactions may be present. Various articles [13–22] and reviews [23,24] have described condensed phase systems in which anions are interacting with the host molecule by mainly multiple hydrogen bonding or by ion–dipole interactions. Similar gas phase systems are fairly rare, and are mainly limited to perfluorinated crown ethers [25] and cryptands [26] binding to F^- or $O_2^{\cdot\,-}$. Larson and McMahon speculated on the possibility of multiple site interactions in $Cl^-((CF_2H)_2O)$ complexes based on $\Delta G°_{298}$ values from exchange equilibria relative to $Cl^-(CF_3OCF_2H)$, studied by ion cyclotron resonance (ICR) spectrometry [27]. No information on standard entropy changes ($\Delta S°$) could be obtained, thus preventing a more definitive proof for the occurrence of chelation. Zhang et al. used pulsed-ionization high-

* Corresponding author. E-mail: mcmahon@Uwaterloo.ca

Dedicated to Professor Dr. N. M. M. Nibbering on the occasion of his retirement from the University of Amsterdam and for his many contributions to gas phase ion chemistry.

PII S1387-3806(01)00404-3

pressure mass spectrometry (PHPMS) to deduce that in chloride ion–diol complexes bidentate interactions take place. This was shown experimentally by the standard entropy changes accompanying the clustering reactions [28]. PHPMS is one of the few experimental techniques able to obtain $\Delta S°$ values for gas phase clustering reactions, and excellent examples that illustrate the use of $\Delta S°$ can be found in work by Norrman and McMahon [29,30]. From different $\Delta S°$ values, obtained by deconvoluting the relevant Van't Hoff plots, they showed the existence of low and high temperature isomers for the gas phase clustering of $t\text{-}C_4H_9^+$ onto various small organic molecules [29], and the folding of $CH_3(CH_2)_8CO_2^-$ to give intramolecular solvation [30]. In the present work, the clustering of chloride ion onto various (fluorinated) ethers has been investigated by PHPMS and high-level ab initio computational methods. By varying the number and the positions of the electronegative fluorine atoms, one would expect changes in the structures of the cluster ions, accompanied by changes in the clustering thermochemistry. The computations were performed to obtain more insight into the structures, especially where various rotamers and isomers are possible, and to find a method to compare the thermochemistry to experiment. Recently there has been a fair amount of interest in fluorinated ethers [31–41]. This class of compounds has been developed to replace chlorofluorocarbons (CFCs). Unfortunately these compounds may also contribute to global warming by their long atmospheric lifetimes, and their strong absorption of thermal radiation between 800 and 1400 cm^{-1} [36]. The occurrence of the chloride ion–fluorinated ether complexes in the atmosphere, and especially the ionosphere, seems very unlikely, mainly due to the low concentrations of both chloride ions and the fluorinated ethers at those altitudes.

2. Experimental

All measurements were carried out on a PHPMS instrument, configured around a VG 8-80 mass spectrometer. The instrument, constructed at the University of Waterloo, has been described in detail previously [42]. The general principles and capabilities, as well as the limitations of PHPMS have been described in the literature [43,44].

Gas mixtures were prepared in a 5 L heated stainless steel reservoir at 370 K, by using CH_4 as a bath gas at pressures of 40–900 Torr. Chloride ion was generated from trace amounts of CCl_4 by dissociative electron capture (DEC) of thermalized electrons from 500 μs pulses of a 2 keV electron gun beam.

The five ethers ($(CH_3)_2O$, $(CH_3CH_2)_2O$, CH_3OCF_3, $(CF_2H)_2O$, and CF_3OCF_2H) were added to give relative amounts between 0.06% and 75%, depending on the ion source temperature and the nature of the experiment involved. The ion source pressure and temperature ranged from 4.0 to 8.0 Torr and from 300 to 600 K, respectively.

Time intensity profiles of mass selected ions were monitored by using a PC based multichannel scalar (MCS) data acquisition system, configured between 60 and 200 μs dwell time per channel over 250 channels. Additive accumulations of ion signals resulting from 500 to 2000 electron gun beam pulses were typically used. Fig. 1(a) and (b) illustrate typical data obtained from the equilibrium experiments.

Equilibrium constants (K_{eq}) at different absolute temperatures for the various chloride ion–ether clustering equilibria, $Cl^- + \text{ether} \rightleftharpoons Cl^-(\text{ether})$, are determined from

$$K_{eq} = \frac{\text{Int}(Cl^-(\text{ether}))}{\text{Int}(Cl^-)} \frac{P^0}{P_{\text{ether,source}}} \quad (1)$$

In Eq. (1) $\text{Int}(Cl^-(\text{ether}))/\text{Int}(Cl^-)$ is the ion intensity ratio of the $Cl^-(\text{ether})$ and Cl^- ions at equilibrium, P^0 is the standard pressure (1 atm), and $P_{\text{ether,source}}$ is the partial pressure (in atm) of the ether in the ion source.

From the equilibrium constants the standard Gibbs' free energy change ($\Delta G°$) at different absolute temperatures (T) can be calculated from

$$\Delta G° = -RT \ln(K_{eq}) \quad (2)$$

By combining Eq. (2) and the following equation:

$$\Delta G° = \Delta H° - T\Delta S° \quad (3)$$

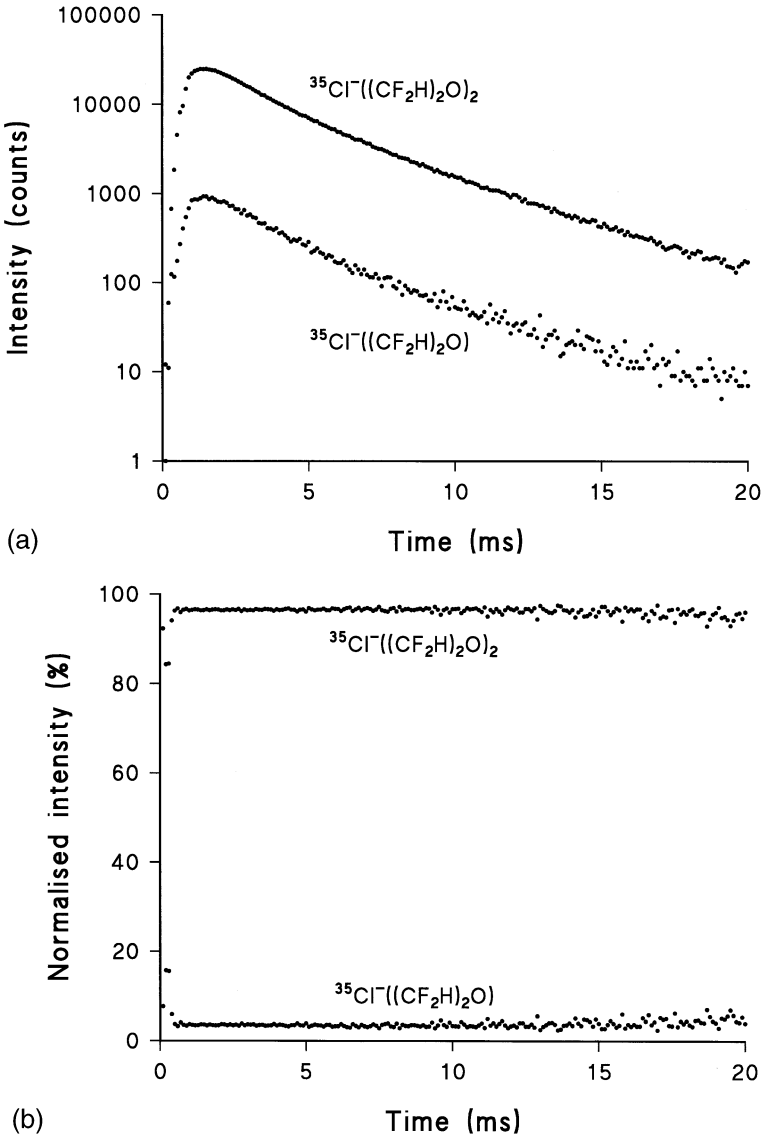

Fig. 1. (a) Time-intensity profile for the $Cl^-((CF_2H)_2O)+(CF_2H)_2O \rightleftharpoons Cl^-((CF_2H)_2O)_2$ clustering equilibrium at the following experimental conditions: $P_{\text{ion source}} = 4.00$ Torr, $T_{\text{ion source}} = 352$ K, $P(CH_4) = 3.97$ Torr, $P((CF_2H)_2O) = 0.03$ Torr, $P(CCl_4) \ll 0.01$ Torr. (b) Normalized time-intensity profile of (a).

the Van't Hoff equation,

$$\ln(K_{eq}) = \frac{\Delta S^\circ}{R} - \frac{\Delta H^\circ}{R}\frac{1}{T} \quad (4)$$

can be obtained.

By plotting $\ln(K_{eq})$ versus $1/T$, ΔH° and ΔS° can be obtained from the slope and intercept, respectively. All equilibrium constants obtained were essentially independent of the partial pressures of the various ethers and the ion source pressure.

Dimethyl ether was obtained from Matheson of Canada Ltd., diethyl ether from BDH Inc., 1,1,1-trifluoro dimethyl ether and 1,1,1,3,3-pentafluoro dimethyl ether from Syn Quest Labs Inc., 1,1,3,3-

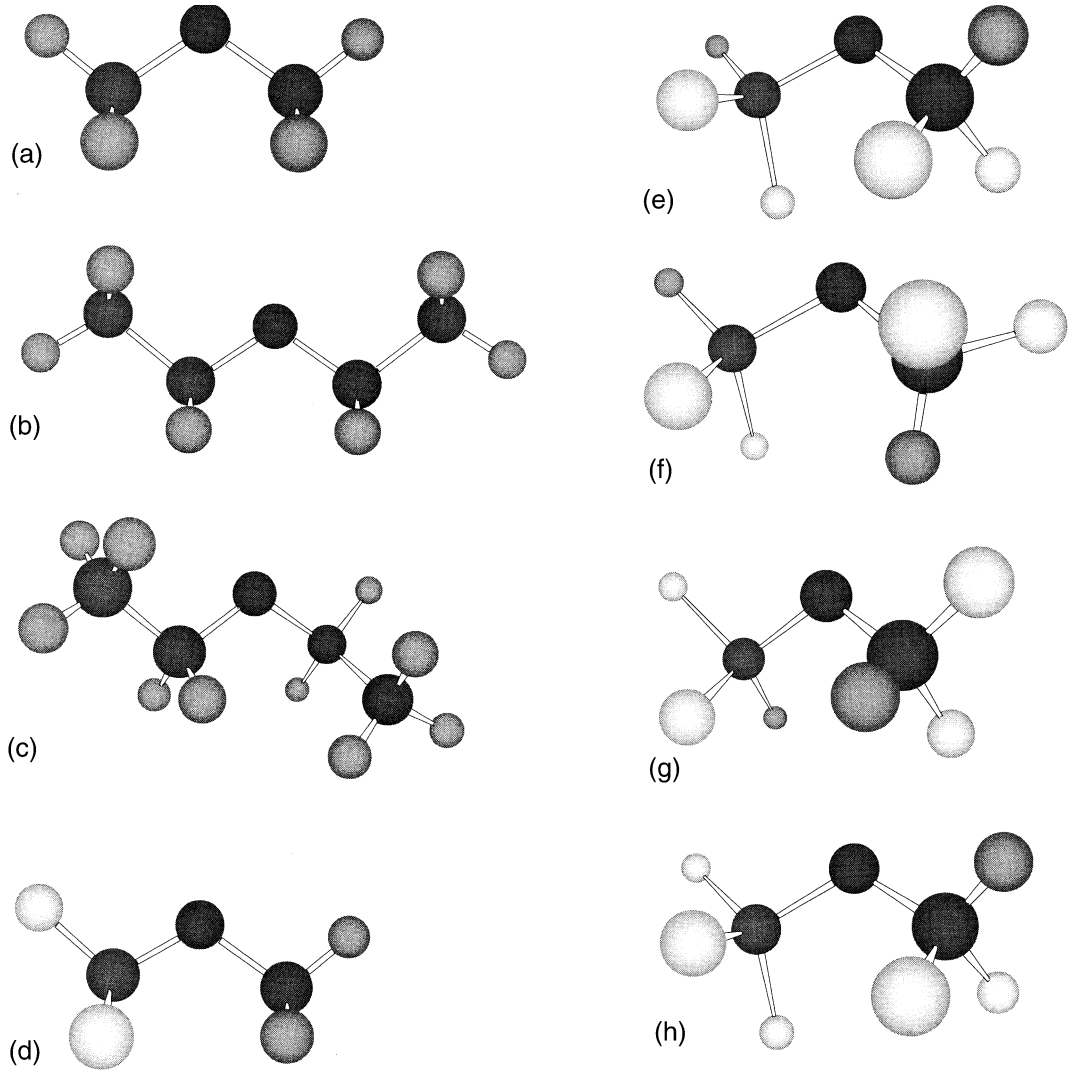

Fig. 2. Optimized MP2/6-31G(*d*) structures of (a) $(CH_3)_2O$, (b) $(CH_3CH_2)_2O$ (rotamer 1), (c) $(CH_3CH_2)_2O$ (rotamer 2), (*d*) CH_3OCF_3, (e) $(CF_2H)_2O$ (rotamer 1), (f) $(CF_2H)_2O$ (rotamer 2), (g) $(CF_2H)_2O$ (rotamer 3), (h) CF_3OCF_2H (rotamer 1), (i) CF_3OCF_2H (rotamer 2), and (j) $(CF_3)_2O$.

tetrafluoro dimethyl ether from PCR Research Chemicals Inc., methane from Praxair, and carbon tetrachloride from J. T. Baker Chemical Co. All chemicals were used as received.

3. Computational

All computations were performed using the GAUSSIAN 98W suite of programs [45]. Geometries were optimized at the Hartree-Fock (HF) [46] and second-order Møller-Plesset perturbation theory (MP2(fc)) [47] levels of theory using the 6-31G(*d*) (**1**) basis set for C, H, O, and F, and the 6-31 + G(*d*) (**3**) basis set for Cl. Normal mode vibrational frequencies were calculated at the HF level of theory and scaled by 0.8953 [48], using the same basis sets as for the HF geometry optimizations. Single point energy and natural population analysis (NPA) [49] calculations were performed at the MP2 level of theory using the 6-311 + G(2*df,p*) (**2**) basis set for C, H, O, and

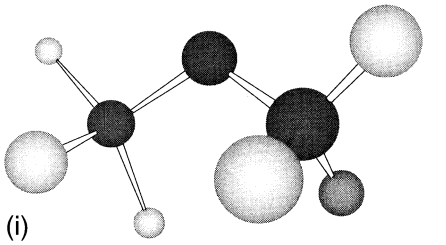

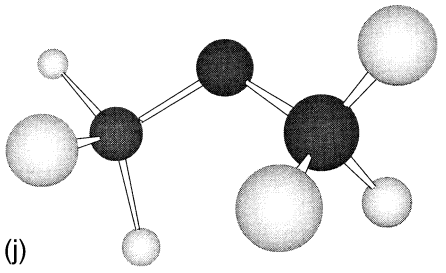

Figure 2. (*continued*)

F, and the 6-311 ++ G(3*df*,3*pd*) (**4**) basis set for Cl on the MP2 geometries.

The motivation to use the 6-31G(*d*) basis set for C, H, F, and O in HF geometry optimizations and frequency calculations, and MP2 geometry optimizations, and the use of the 6-311 + G(2*df*,*p*) basis set for MP2 single point calculations is mainly based on the work by East and Radom [50]. For a fairly large number of molecules they determined that experimental methyl group rotational barriers could accurately be reproduced by using the MP2/6311 + G(2*df*,*p*)// MP2/6-31G(*d*) level of theory. Since there was some interest a priori to also look at the effect of clustering on methyl group barrier heights, it seemed a logical choice to use a similar method.

The choice of 6-311 ++ G(3*df*,3*pd*) as the Cl^- basis set for the MP2 single point calculations is due to the smallest difference in EA($Cl^{\cdot}$) between theory and experiment (3.54 eV versus 3.6144 eV) [51]. For the HF geometry optimizations and frequency calculations, and the MP2 geometry optimizations the use of 6-31 + G(*d*) as the Cl^- basis set was mainly determined by cost considerations. Use of, for instance 6-31 ++ G(*d*) or 6-31 ++ G(*d*,*p*), does not improve the value of the calculated EA($Cl^{\cdot}$)'s, which show large discrepancies with the experimental EA (2.48 eV for HF and 3.16 eV for MP2).

G3(MP2) [52] enthalpies, $H°_{298}$(G3(MP2)), were calculated for Cl^-, CH_3OCF_3, CF_3O^-, CH_3Cl, $Cl^-(CH_3OCF_3)$, $CF_3O^-(CH_3Cl)$, and $[ClCH_3OCF_3]^-$ to construct a schematic energy profile for the $Cl^- + CH_3OCF_3 \rightarrow CF_3O^- + CH_3Cl$ gas phase S_N2 reaction.

4. Results and discussion

4.1. Structures

The MP2/1 structures of the various rotamers of $(CH_3)_2O$, $(CH_3CH_2)_2O$, CH_3OCF_3, $(CF_2H)_2O$, CF_3OCF_2H, and $(CF_3)_2O$ are shown in Fig. 2(a)–(j). Recently, results of optimized structures for several of the same molecules, but only the most stable rotamers, calculated at the MP2 and QCISD/6-31G(*d*), and B3LYP/6-311 ++ G(3*df*,3*pd*) levels of theory were published [36–38]. For a discussion on the structural features of $(CH_3)_2O$ calculated at the MP2/6-31G(*d*) level of theory versus experiment the reader is referred to recent work by Good and Francisco [36]. For $(CH_3CH_2)_2O$ no systematic study of the various rotamers was performed. For $(CF_2H)_2O$ and CF_3OCF_2H, four and two stable conformers were found, respectively. Unfortunately, no microwave or electron diffraction experiments have been performed on the fluorinated ethers to determine the most stable structures and the possible existence of the various rotamers. Calculations on $(CF_3)_2O$ at the MP2/3-21G and MP2/6-31G(*d*,*p*) levels of theory show good agreement with this work [37,38]. $(CF_3)_2O$ shows an eclipsed structure to minimize the repulsion among the fluorine atoms. A dihedral angle, ∠ FCCF, of 46.8° between the two axial fluorine atoms and the two carbon atoms was found. More interestingly, from the point of view of the work presented here, are the structures of the chloride ion–ether complexes, which are shown in Fig. 3(a)–(k). Smith et al. published a structure for the $Cl^-((CH_3)_2O)$ complex, calculated at the MP2/[D95 + */D95 + **] level of

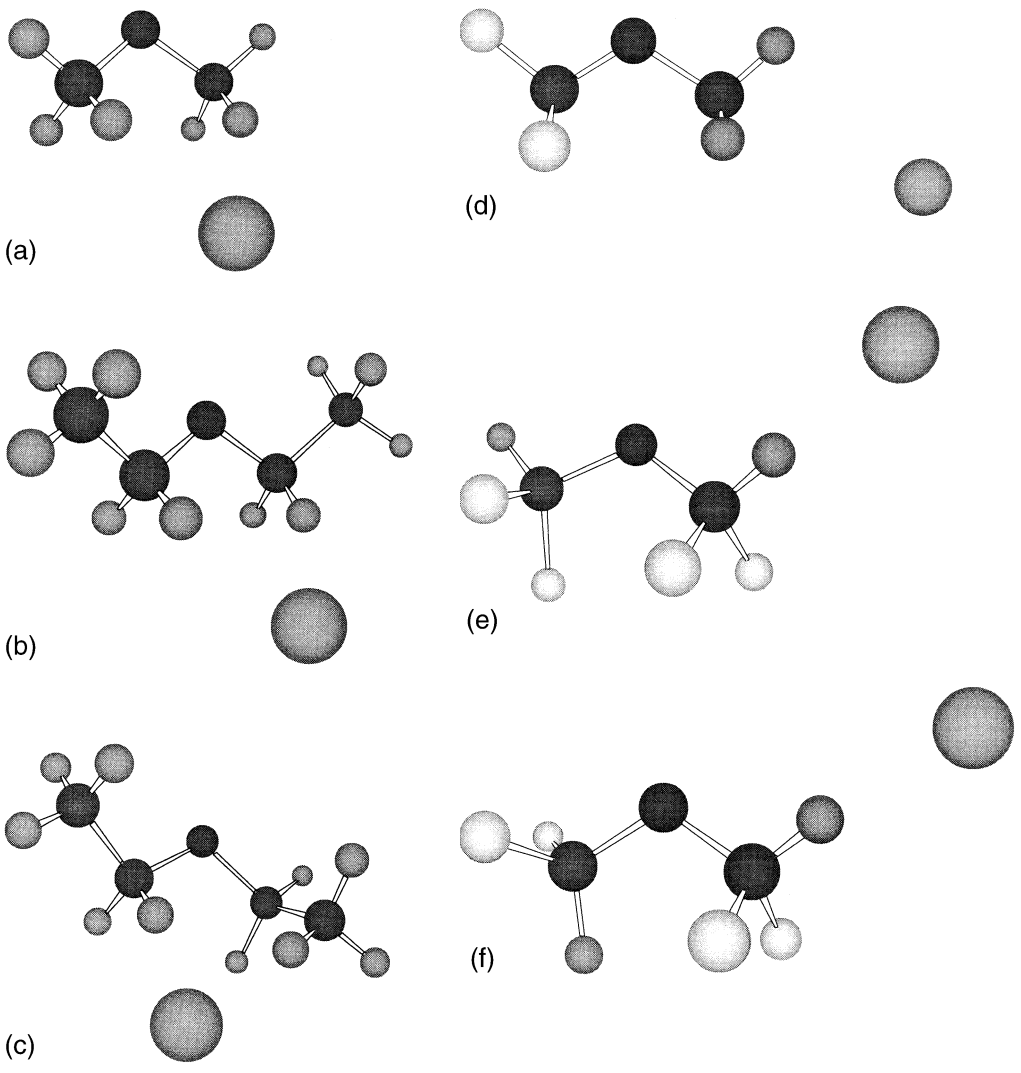

Fig. 3. Optimized MP2/[6-31 + G(*d*)/6-31G(*d*)] structures of (a) $Cl^-((CH_3)_2O)$, (b) $Cl^-((CH_3CH_2)_2O)$ (rotamer 1), (c) $Cl^-((CH_3CH_2)_2O)$ (rotamer 2), (*d*) $Cl^-(CH_3OCF_3)$, (e) $Cl^-((CF_2H)_2O)$ (rotamer 1), (f) $Cl^-((CF_2H)_2O)$ (rotamer 2, isomer 1), (g) $Cl^-((CF_2H)_2O)$ (rotamer 2, isomer 2), (h) $Cl^-((CF_2H)_2O)$ (rotamer 4), (i) $Cl^-(CF_3OCF_2H)$ (rotamer 1), (j) $Cl^-(CF_3OCF_2H)$ (rotamer 2), and (k) $Cl^-((CF_3)_2O)$.

theory [53]. In the most stable isomers of $Cl^-((CH_3)_2O)$ found in this work, the chloride ion interacts with only two hydrogen atoms, one from each methyl group. The Cl^-–H distance is 2.795 Å, which is much smaller than the 3.2 Å found by Smith et al., which appears to be a transition state structure, since the chloride ion interacts with four hydrogen atoms [53]. Upon complex formation with Cl^-, the C–O–C angle remains virtually unchanged. For the chloride ion–diethyl ether complex, at least two isomers are possible. In the first one, the chloride ion interacts with two hydrogen atoms from the two CH_2 units, while in the second isomer the chloride ion interacts with two hydrogens, one from a CH_2 and the other from a CH_3 unit on different sides of the oxygen atom. The calculated thermochemistry for the latter isomer has closer agreement to the experimental PHPMS data. No isomer was found where the chloride ion

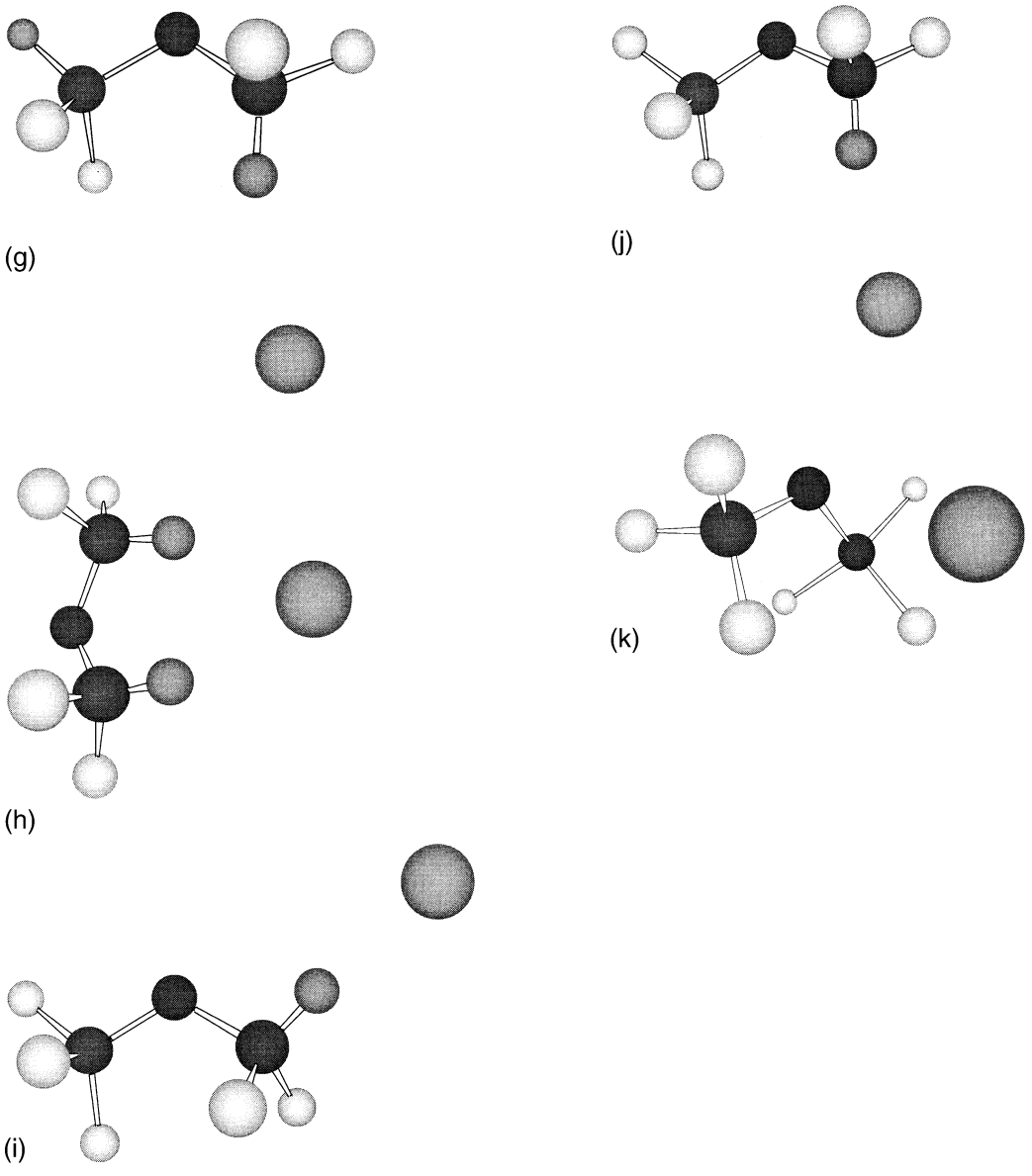

Figure 3. (*continued*)

interacts with hydrogen atoms from the two CH_3 units. The introduction of a CF_3 group changes the chloride ion binding as expected. $Cl^-(CH_3OCF_3)$ looks like a S_N2 back-side attack complex. Relative to CH_3OCF_3, the O–CH_3 distance increases from 1.442 to 1.472 Å, whereas the O–CF_3 distance decreases from 1.345 to 1.328 Å. However, the chloride ion does not interact identically with all hydrogen atoms, as occurs, for instance in the $Cl^-(CH_3Cl)$ complex. In $Cl^-(CH_3OCF_3)$ the Cl^-CO bond angle is 171.5°, whereas the COC bond angle is 115.2°, compared to 114.4° in CH_3OCF_3. For the $Cl^-((CF_2H)_2O)$ cluster, four different rotamers/isomers are possible, three sin-

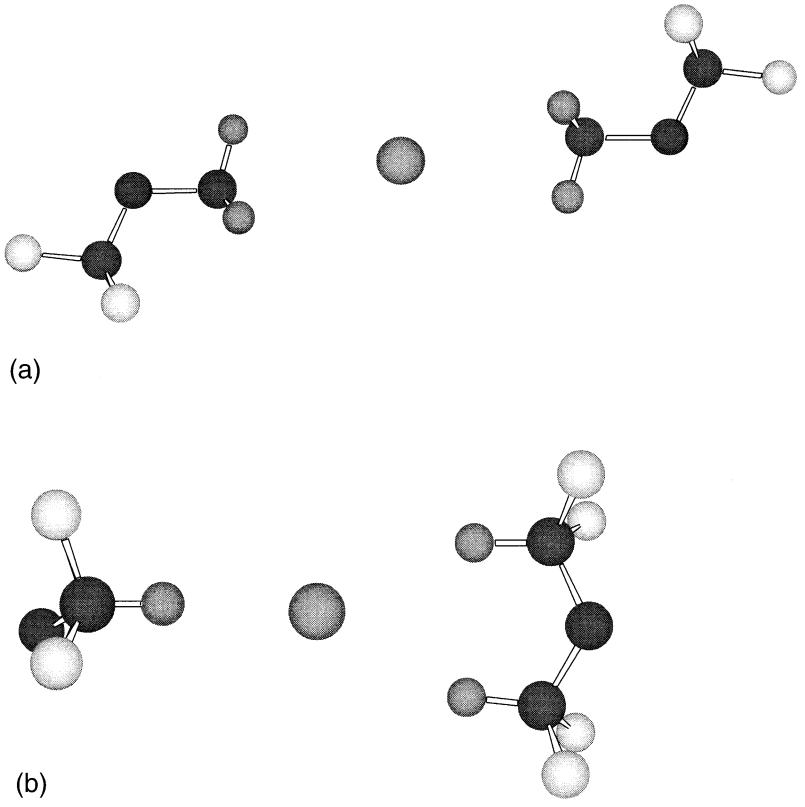

Fig. 4. Optimized MP2/[6-31+G(*d*)/6-31G(*d*)] structures of (a) $Cl^-(CH_3OCF_3)_2$, and (b) $Cl^-((CF_2H)_2O)_2$.

gly hydrogen bonded, and one doubly hydrogen bonded. Rotamers 1 and 2 (2 isomers) all have the chloride ion interacting with one of the two hydrogen atoms. Compared to rotamer 4, both the Cl^-–H distances and Cl^-HC bond angles are smaller and are closer to being linear, respectively. In rotamer 4, there is not only interaction with two hydrogen atoms, but the chloride ion is also aligned with the dipole moment of $(CF_2H)_2O$. For the $Cl^-(CF_2HOCF_3)$ cluster, two rotamers are possible. In both cases the Cl^-HC bond angle is close to being linear. In most clusters investigated, the C–O bond containing the hydrogen atom that interacts with the chloride ion increases in length relative to the neutral, while the C–O bond with no hydrogen atom(s) interacting decreases in length. In $Cl^-((CF_3)_2O)$ the FCCF dihedral angle, containing the axial fluorine atoms, has been reduced to 39.7°. More interesting is the fact that the chloride ion interaction with the carbon atom is an almost linear alignment with one of the C–F bonds. This resembles a S_N2 back side attack complex of Cl^- with $(CF_3)_2O$, with F^- as a hypothetical leaving group instead of CF_3O^-. The Cl^-–C distance is 3.775 Å, which is notably longer than the Cl^-–O distance of 3.322 Å. The NPA charges in $(CF_3)_2O$, calculated at the MP2/6-311+G(2*df*,*p*)//MP2/6-31G(*d*) level of theory, confirm that the carbon atom will be the only probable site the chloride ion can interact with. The two di-solvated chloride ion-fluorinated ether complexes shown in Fig. 4(a) and (b), $Cl^-(CH_3OCF_3)_2$ and $Cl^-((CF_2H)_2O)_2$, show characteristics that are very close to the monosolvated clusters. It is interesting, but not surprising, to note that the hydrogen bonded arrangement around Cl^- in $Cl^-((CF_2H)_2O)_2$ is tetrahedral like. In this way

Table 1
Summary of the experimental thermochemical data for the chloride ion–ether clustering equilibria $Cl^-(ether)_n$ + ether ⇌ $Cl^-(ether)_{n+1}$ (ether = $(CH_3)_2O$, $(CH_3CH_2)_2O$, CH_3OCF_3, $(CF_2H)_2O$, CF_3OCF_2H; n = 0, 1)[a]

Clustering equilibrium	$\Delta H°$ (kcal mol^{-1})	$\Delta S°$ (cal mol^{-1} K^{-1})
Cl^- + CH_3OCH_3 ⇌ $Cl^-(CH_3OCH_3)$	−7.5	−15.3
Cl^- + $C_2H_5OC_2H_5$ ⇌ $Cl^-(C_2H_5OC_2H_5)$	−9.0	−19.1
Cl^- + CH_3OCF_3 ⇌ $Cl^-(CH_3OCF_3)$	−13.6	−19.8
$Cl^-(CH_3OCF_3)$ + CH_3OCF_3 ⇌ $Cl^-(CH_3OCF_3)_2$	−12.7	−23.7
Cl^- + CF_2HOCF_2H ⇌ $Cl^-(CF_2HOCF_2H)$	−28.2	−31.3
$Cl^-(CF_2HOCF_2H)$ + CF_2HOCF_2H ⇌ $Cl^-(CF_2HOCF_2H)_2$	−21.4	−33.7
Cl^- + CF_2HOCF_3 ⇌ $Cl^-(CF_2HOCF_3)$	−17.5	−20.8

[a] Estimated relative errors: $\Delta H°$ ± 0.2 kcal mol^{-1}; $\Delta S°$ ± 1.0 cal mol^{-1} K^{-1} and estimated absolute errors: $\Delta H°$ ± 0.4 kcal mol^{-1} $\Delta S°$ ± 2.0 cal mol^{-1} K^{-1}

the repulsive interaction between the two $(CF_2H)_2O$ molecules is minimized. Compared to $Cl^-((CF_2H)_2O)$, the Cl^-–H distances have slightly increased, from around 2.436 to 2.470 Å.

4.2. Thermochemistry

In Tables 1 and 2, overviews are given of the experimental and computational thermochemical data obtained for the chloride ion–(fluorinated) ether complex clustering equilibria. As can be seen from Table 1, the $\Delta H°$ and $\Delta S°$ values depend very much on the number of fluorine atoms and the substitution pattern. In Figs. 5 and 6, the Van't Hoff plots from which the $\Delta H°$ and $\Delta S°$ values are determined are shown. As seen in Fig. 2(a)–(k), very different bonding characteristics can be observed in the various chloride ion–(fluorinated) ether complexes, which should be reflected in characteristic $\Delta H°$ and $\Delta S°$ values. PHPMS is one of the few experimental techniques to obtain $\Delta S°$ values directly, and these can be a very useful tool to assign structural features of gas phase cluster ions. The $\Delta H°$ and $\Delta S°$ values for chloride ion

Table 2
Summary of the computational thermochemical data for the chloride ion–ether clustering equilibria $Cl^-(ether)_n$ + ether ⇌ $Cl^{-1}(ether)_{n+1}$ (ether = $(CH_3)_2O$, $(CH_3CH_2)_2O$, CH_3OCF_3, $(CF_2H)_2O$, CF_3OCF_2H, $(CF_3)_2O$; n = 0, 1)[a]

Clustering equilibrium	$\Delta H_{298}°$ (kcal mol^{-1}) MP2//MP2	$\Delta S_{298}°$ (cal mol^{-1} K^{-1}) HF
Cl^- + $(CH_3)_2O$ ⇌ $Cl^-((CH_3)_2O)$ (rotamer 1)	−7.3	−15.8
Cl^- + $(CH_3CH_2)_2O$ ⇌ $Cl^-((CH_3CH_2)_2O)$ (rotamer 1)	−7.8	−15.7
Cl^- + $(CH_3CH_2)_2O$ ⇌ $Cl^-((CH_3CH_2)_2O)$ (rotamer 2)	−8.9	−17.6
Cl^- + CH_3OCF_3 ⇌ $Cl^-(CH_3OCF_3)$ (rotamer 1)	−12.5	−17.2
$Cl^-(CH_3OCF_3)$ + CH_3OCF_3 ⇌ $Cl^-(CH_3OCF_3)_2$ (rotamer1)	−10.6	−12.4
Cl^- + $(CF_2H)_2O$ ⇌ $Cl^-((CF_2H)_2O)$ (rotamer 1)	−14.4	−18.8
Cl^- + $(CF_2H)_2O$ ⇌ $Cl^-((CF_2H)_2O)$ (rotamer 2, isomer 1)	−12.4	−17.7
Cl^- + $(CF_2H)_2O$ ⇌ $Cl^-((CF_2H)_2O)$ (rotamer 2, isomer 2)	−16.1	−19.0
Cl^- + $(CF_2H)_2O$ ⇌ $Cl^-((CF_2H)_2O)$ (rotamer 4)	−24.5	−20.2
$Cl^-((CF_2H)_2O)$ + $(CF_2H)_2O$ ⇌ $Cl^-((CF_2H)_2O)_2$ (rotamer 4)	−18.7	−17.7
Cl^- + CF_3OCF_2H ⇌ $Cl^-(CF_3OCF_2H)$ (rotamer 1)	−17.3	−19.5
Cl^- + CF_3OCF_2H ⇌ $Cl^-(CF_3OCF_2H)$ (rotamer 2)	−17.6	−19.8
Cl^- + $(CF_3)_2O$ ⇌ $Cl^-((CF_3)_2O)$ (rotamer 1)	−4.9	−16.0

[a] $\Delta H_{298}°$: MP2(fc)/[**2**/**4**]//MP2(fc)/[**1**/**3**] + (ZPE + ΔC_P(298.15 K) + RT) (HF/[**1**/**3**]) (0.8953) and $\Delta S_{298}°$: HF/[**1**/**3**] (0.8953), and $\Delta S_{298}°$: HF/[**1**/**3**] (0.8953), where **1** = 6-31G(*d*), **2** = 6-311+G(2*df*,*p*), **3** = 6-31+G(d), **4** = 6-311++G(3*df*,3*pd*); **1** and **2** for C, H, F, and O and **3** and **4** for Cl^-.

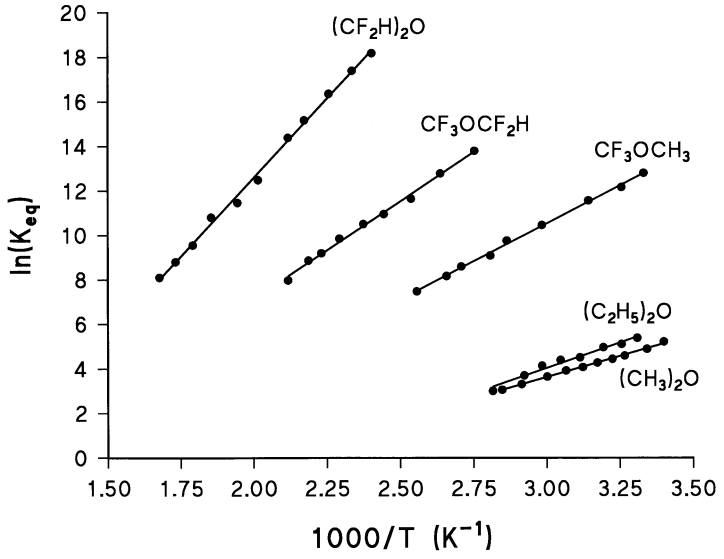

Fig. 5. Van't Hoff plots for the chloride ion–ether clustering equilibria $Cl^- + ether \rightleftharpoons Cl^-(ether)$ (ether = $(CH_3)_2O$, $(CH_3CH_2)_2O$, CH_3OCF_3, $(CF_2H)_2O$, CF_3OCF_2H).

binding to dimethyl and diethyl ether can be compared to data obtained recently in our laboratory on chloride ion binding to cyclic and linear alkanes [54]

$$Cl^- + RH \rightleftharpoons Cl^-(RH) \quad (5)$$

For RH = *c*-C_5H_{10} and *n*-C_5H_{12}, $\Delta H°$ and $\Delta S°$ values of −7.4 and −7.9 kcal mol^{-1}, and −16.4 and −18.1 cal mol^{-1} K^{-1}, respectively, were determined. These values seem reasonable for the weak, mainly ion-induced dipole, interactions in these types of clusters.

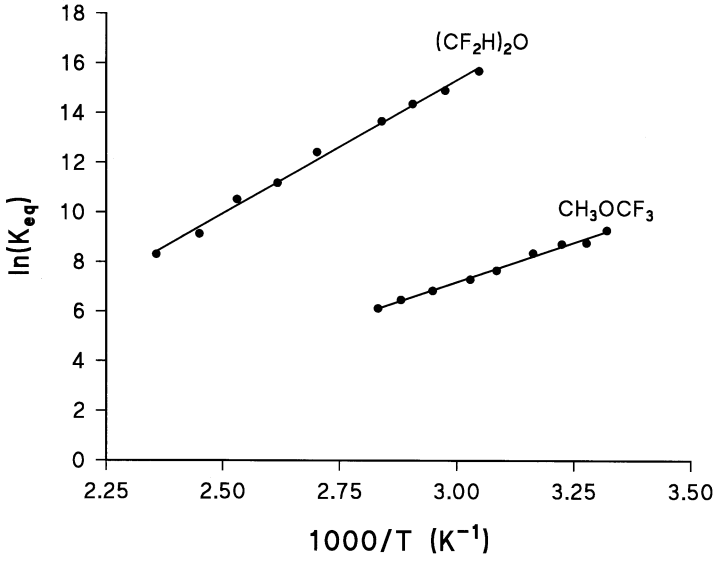

Fig. 6. Van't Hoff plots for the chloride ion–ether clustering equilibria $Cl^-(ether) + ether \rightleftharpoons Cl^-(ether)_2$ (ether=CH_3OCF_3, $(CF_2H)_2O$).

The difference between $(CH_3)_2O$ and $(CH_3CH_2)_2O$ is mainly due to a larger polarizability of the latter ($\alpha = 5.8$ Å^3 versus 10.2 Å^3) [55]. Smith et al. calculated the complexation energy of Cl^- onto $(CH_3)_2O$ and found a value of -6.90 kcal mol^{-1}, after correcting for the basis set superposition error (BSSE), at the MP2/[cc-pVTZ + 3*s*2*p*2*d*/cc-pVTZ + *sp*]//MP2/[D95 + */D95 + **] level of theory [53]. Rotamer 1 of $(CH_3CH_2)_2O$ is 1.5 kcal mol^{-1} more stable than rotamer 2 ($\Delta H°_{298}$ at the MP2/**2**//MP2/**1** level of theory). For the $Cl^-((CH_3CH_2)_2O)$ complex isomer 1 is only 0.5 kcal mol^{-1} more stable than isomer 2 ($\Delta H°_{298}$ at the MP2/[**2**/**4**]//MP2/[**1**/**3**] level of theory). Existence of other rotamers and isomers cannot, of course, be excluded, and it seems reasonable to assume that the $Cl^-((CH_3CH_2)_2O)$ complexes in the high pressure ion source consist of a statistical mixture of the various rotamers and isomers. The fact that the calculated $\Delta H°_{298}$ and ΔS_{298} values for rotamer 2 are closer to the experimental $\Delta H°$ and $\Delta S°$ values, by no means proves that these are the main structures in the high pressure ion source. This example illustrates that weakly bound systems can be stabilized by multiple, nonclassical hydrogen bonds. It may be expected that this effect will become even more pronounced if the alkyl chain length in CH_3OR (R = alkyl) will increase. One problem that may arise when trying to analyze the experimental $\Delta H°$ and $\Delta S°$ values, is dealing with large numbers of conformers of the neutral ethers and the possible isomers for the chloride ion-ether complexes, that all will have their own, distinct thermochemistry. As already mentioned previously, the $Cl^-(CH_3OCF_3)$ complex resembles a S_N2 backside attack complex, even though the binding is not completely symmetric. For a similar, true S_N2 system,

$$Cl^- + CH_3Br \rightleftharpoons Cl^-(CH_3Br) \quad (6)$$

values for $\Delta H°$ and $\Delta S°$ of -12.5 kcal mol^{-1} and -19.0 cal mol^{-1} K^{-1}, respectively, were determined [56], with the latter obtained from ab initio computations [57].

CF_3O^- was present in the ion source, and from the potential energy surface calculated at the G3(MP2) level of theory, shown in Fig. 7, it seems reasonable to assume that it has been formed by a S_N2 type reaction

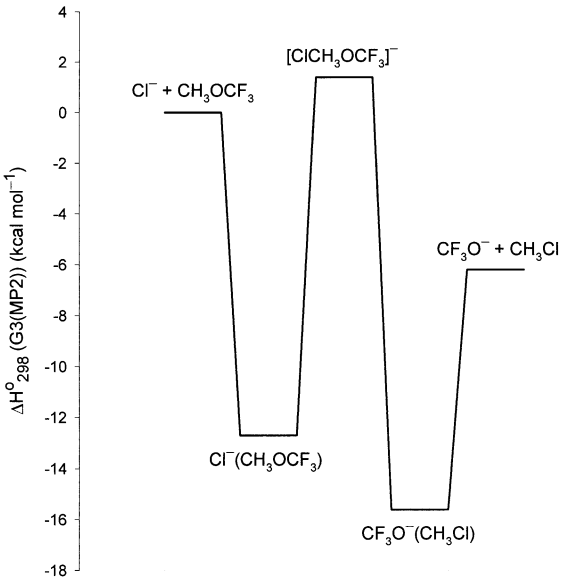

Fig. 7. Schematic G3(MP2) energy profile for the $Cl^- + CH_3OCF_3 \rightarrow CF_3O^- + CH_3Cl$ gas phase S_N2 reaction.

$$Cl^- + CH_3OCF_3 \rightarrow CF_3O^- + CH_3Cl \quad (7)$$

The CF_3O^- formed can also cluster with CH_3OCF_3, forming $CF_3O^-(CH_3OCF_3)$. The latter ion is present in a very small intensity, but nonetheless equilibrium was observed. The standard ambient reaction enthalpy change, $\Delta_R H°_{298}$, calculated at the G3(MP2) level of theory is -6.2 kcal mol^{-1}, whereas the experimental value is -5.9 kcal mol^{-1} [62]. For the latter value, $\Delta_f H°_{298}$ (CH_3OCF_3) of -212.7 kcal mol^{-1} was used, which was calculated at the G2(MP2) level of theory [35]. At the G3(MP2) level of theory a $\Delta_f H°_{298}$ (CH_3OCF_3) value of (-215.7 ± 0.1) kcal mol^{-1} has been determined. Computations at the G3(MP2) level of theory indicate that the $[ClCH_3OCF_3]^-$ transition state is 1.4 kcal mol^{-1} above the Cl^- and CH_3OCF_3 reactants. At the same level of theory, the $\Delta H°_{298}$ values for

$$Cl^- + CH_3OCF_3 \rightleftharpoons Cl^-(CH_3OCF_3) \quad (8)$$

$$CF_3O^- + CH_3Cl \rightleftharpoons CF_3O^-(CH_3Cl) \quad (9)$$

were calculated to be -12.7 kcal mol^{-1} and -9.4 kcal mol^{-1}, respectively.

The first result is in excellent agreement with the MP2//MP2 calculations reported here. It does not seem unlikely that CF_3O^- is formed through dissociative electron capture by CF_3OCH_3

$$CH_3OCH_3 + e^- \rightarrow [CF_3OCH_3]^{\cdot -} \rightarrow$$

$$CF_3O^- + CH_3^{\cdot} \quad (10)$$

Electron radiolysis of CF_3OCH_3 into $CF_3O^{\cdot}$ and $CH_3^{\cdot}$, followed by electron capture by $CF_3O^{\cdot}$ also seems a very unlikely process

$$CH_3OCH_3 + e^- \rightarrow CF_3O^{\cdot} + CH_3^{\cdot} + e^- \quad (11)$$

$$CF_3O^{\cdot} + e^- \rightarrow CF_3O^- \quad (12)$$

The first process is 95.7 kcal mol^{-1} endothermic [58] (96.3 kcal mol^{-1} at the G3(MP2) level of theory), whereas the second process is 101.2 kcal mol^{-1} exothermic [58] (104.5 kcal mol^{-1} at the G3(MP2) level of theory), making the overall process 5.5 exothermic (8.2 kcal mol^{-1} at the G3(MP2) level of theory). The probability of the two-step process is low, because of low concentrations of the species involved.

Larson and McMahon measured $\Delta G°_{298}$ for $Cl^- + (CF_2H)_2O \rightleftharpoons Cl^-((CF_2H)_2O)$ (-17.0 kcal mol^{-1}) and $Cl^- + CF_3OCF_2H \rightleftharpoons Cl^-(CF_3OCF_2H)$ (-12.1 kcal mol^{-1}) by ICR, from exchange equilibria with various chloride ion clusters [27]. From the present PHPMS data, $\Delta G°_{298}$ values of (-18.8 ± 1.0) kcal mol^{-1} and (-11.3 ± 1.0) kcal mol^{-1} can be determined, in reasonable to good agreement with the ICR values. The relatively negative $\Delta H°$ and $\Delta S°$ values for the $Cl^- + (CF_2H)_2O \rightleftharpoons Cl^-((CF_2H)_2O)$ equilibrium seems very reasonable. Zhang et al. measured, by PHPMS, the thermochemistry for the $Cl^- + HO(CH_2)_3OH \rightleftharpoons Cl^-(HO(CH_2)_3OH)$ equilibrium, and found $\Delta H°$ and $\Delta S°$ values of (-28.3 ± 1.7) kcal mol^{-1} and (-34.0 ± 0.7) cal mol^{-1} K^{-1}, respectively [28]. The $\Delta H°$ value for the $Cl^- + CF_3OCF_2H \rightleftharpoons Cl^-(CF_3OCF_2H)$ equilibrium of -17.5 kcal mol^{-1}, is equal to the $\Delta H°$ value for chloride ion binding onto methanol [59]. The difference in $\Delta S°$ values for these two equilibria is mainly due to the fact that in the $Cl^-(HOCH_3)$ cluster, Cl^- has some interaction with two methyl group hydrogen atoms, making the latter one more negative due to hindering of the methyl group rotation. In rotamer 1 of $Cl^-(CF_3OCF_2H)$ there is no hindering of the CF_3 group rotation expected, thus giving a possible explanation for the less negative $\Delta S°$ value. In general, it is expected that multiple hydrogen bonding will be thermodynamically more favorable than single. If one compares the $\Delta H°$ and $\Delta S°$ values for formation of $Cl^-((CF_2H)_2O)$ (double hydrogen bonding) and $Cl^-(CF_3OCF_2H)$ (single hydrogen bonding), one can make an estimate of the gains in $\Delta H°$ and $\Delta S°$ for going from a single hydrogen in $Cl^-((CF_2H)_2O)$ (rotamers 1 and 2 (isomers 1 and 2)) to a double hydrogen bond in rotamer 4. From the PHPMS data, $\Delta\Delta H°$ and $\Delta\Delta S°$ values of -10.7 kcal mol^{-1} and -10.5 cal mol^{-1} K^{-1}, respectively, can be calculated, thus providing the thermodynamic driving force for chelation. Converting these values to $\Delta\Delta G°_{298}$ (-7.4 kcal mol^{-1}) gives an excellent agreement with the $\Delta\Delta G°_{298}$ value of -7.6 kcal mol^{-1} by Larson and McMahon from their ICR experiments [27]. From the ab initio computations a $\Delta\Delta H°_{298}$ value of -7.4 kcal mol^{-1} can be calculated going from rotamer 2/isomer 2 to rotamer 4 for $Cl^-((CF_2H)_2O)$. It is interesting to note that for $(CF_2H)_2O$ the rotational conformer where the two CF_2H groups are staggered relative to each other is the most stable one, but that the whole picture of the relative stabilities, as it applies to the neutrals, is no longer valid in the chloride ion–ether complex. As expected, formation of two hydrogen bonds will be more favorable than only one. The $\Delta H°$ and $\Delta S°$ values for the two di-solvation equilibria,

$$Cl^-(\text{ether}) + \text{ether} \rightleftharpoons Cl^-(\text{ether})_2 \quad (13)$$

with ether = CH_3OCF_3, $(CF_2H)_2O$), also seem reasonable compared to similar systems reported in literature.

Zhang et al. determined as well the thermochem-

istry for chloride ion clustering on two molecules of 1,3-propanediol,

$$Cl^-(HO(CH_2)_3OH) + HO(CH_2)_3OH \rightleftharpoons Cl^-(HO(CH_2)_3OH)_2 \quad (14)$$

and found $\Delta H°$ and $\Delta S°$ to be (-20.8 ± 0.7) kcal mol^{-1} and (-36.2 ± 0.3) cal mol^{-1} K^{-1}, respectively [28].

The data for $Cl^-((CF_2H)_2O)_2$ show a similar trend as this system, e.g. a decrease in $^-\Delta H°$ of approximately 8 kcal mol^{-1}, and a smaller decrease in $\Delta S°$ of ~2 cal mol^{-1} K^{-1}. Additional hindering of two more CF_2H rotations is the main factor for this larger negative $\Delta S°$ value. In the $Cl^-((CF_2H)_2O)_2$ cluster the bonding to chloride ion is so favorable, that it does seem reasonable that a third $(CF_2H)_2O$ molecule may not interact directly with the chloride ion. Instead, this third solvent molecule will start making up the so-called second solvation shell. If that is actually true, hydrogen bonds may be possible. The two that are most likely to occur would have one, or maybe both, hydrogen atom(s) interacting with either a fluorine atom, CF_2HOCF_2–H · · · F–$CFHOCF_2H$, or the oxygen atom, CF_2HOCF_2–H · · · $O(CF_2H)_2$. It may then be expected that the $\Delta H°$ and $\Delta S°$ values for the $Cl^-((CF_2H)_2O)_2 + (CF_2H)_2O \rightleftharpoons Cl^-((CF_2H)_2O)_3$ clustering equilibria will be substantially less negative than for the mono- and di-solvation equilibria.

4.3. Experiments versus computations

In general, the agreement between the PHPMS data for $\Delta H°$ and computational data for $\Delta H°_{298}$ is very close, thus adding to the confidence in the experimental data. From the computational data it became evident that single point computations using large basis sets were absolutely necessary to obtain reliable $\Delta H°_{298}$ values. It seems that for $(CH_3)_2O$, CH_3OCF_3, and CF_3OCF_2H, the HF level of theory in combination with moderate basis sets like 6-31+G(*d*) for Cl, and 6-31G(*d*) for C, H, F, and O perform well enough to obtain $\Delta S°_{298}$ values that are relatively close to the $\Delta S°$ values from PHPMS. Large disagreement is observed, however especially for $Cl^- + (CF_2H)_2O \rightleftharpoons Cl^-((CF_2H)_2O)$. The very large negative $\Delta S°$ value indicates locking of the CF_2H group rotations upon complexation with Cl^-. Similar values have been obtained for chloride ion clustering with a series of diols, where bidentate interactions occur [28]. GAUSSIAN 98 treats the CH_3, CF_3, and CF_2H group torsional motions as harmonic vibrations. It would be more accurate to treat these as hindered rotations. Work by East and Radom on third-law gas-phase statistical entropies from ab initio computations seems a proper approach to model $\Delta S°$ more accurately [50]. This approach has been applied successfully by De Turi and Ervin to fluoride ion–alcohol complexes [60]. Applying this method to the $Cl^-((CF_2H)_2O)$ system would be very computationally expensive and beyond the scope of this work. Another source of discrepancy between the experimental PHPMS $\Delta S°$ and the computational $\Delta S°_{298}$ values is the anharmonicity of the intramolecular normal mode vibrations. Especially for the two disolvated systems investigated, $Cl^-(CH_3OCF_3)_2$ and $Cl^-((CF_2H)_2O)_2$, many normal mode vibrational frequencies smaller than 200 cm^{-1} are calculated, that all contribute largely to the vibrational entropy.

4.4. Vibrational frequencies

Recently Good and Francisco measured the Fourier transform infrared (FTIR) spectra of the three fluorinated ethers and calculated the normal mode vibrational frequencies at various levels of theory [36]. The best agreement (rms error of 2.7%) was obtained at the B3LYP/6-311 + + G(3*df*,3*pd*) level of theory, and these results were used to assign the various modes. The HF/6-31G(*d*) results scaled by 0.8953 in general agree very well. Upon complexation with chloride ion three new, intramolecular normal mode vibrations are introduced, and both red- and blueshifts are observed for the other vibrations already present the neutral. There is no clear correlation between the shift in C–H normal mode vibrations, $\Delta\nu$(C–H), and $\Delta H°_{298}$, as was recently observed for $\Delta\nu$(RO–H) in X^-(HOR) clusters (X = F, Cl, Br, I; R = CH_3, CH_3CH_2, $(CH_3)_2CH$, $(CH_3)_3C$) [61]. Vibrational predissociation spectroscopy (VPDS) would

be an excellent tool to investigate the C–H stretches in the different Cl^-(ether) complexes and this would test the accuracy of the computations [62]. The various, stable rotational conformers each have a unique set of normal mode vibrational frequencies.

4.5. *Rotational barriers*

For CH_3OCF_3, rotational barriers of 1.20 kcal mol^{-1} (CH_3) and 3.08 kcal mol^{-1} (CF_3) were calculated at the MP2/2//MP2/1 levels of theory. In the $Cl^-(CH_3OCF_3)$ complex, rotational barriers of 1.02 kcal mol^{-1} (CH_3) and 2.87 kcal mol^{-1} (CF_3) were calculated at the MP2/[2/4]//MP2/[1/3] level of theory.

Recently, Good and Francisco calculated the rotational barriers for the methyl groups in $(CH_3)_2O$, CH_3OCF_3, $(CF_2H)_2O$, and CF_3OCF_2H at the B3LYP/6-311 + + (3*df*,3*pd*) level of theory [36]. Values of 2.4, 1.1, 3.6, and 2.9 kcal mol^{-1}, respectively, were obtained. Except for $(CH_3)_2O$ [63], no experimental microwave data are available. In reality, the rotations of the CH_3, CF_3, and CF_2H groups in the four molecules will most likely show coupling of both methyl groups present. This will give rise to complicated two-dimensional potential energy surfaces. Very little theoretical work has been published on the influence of complex formation on barrier heights of methyl group rotations. De Turi and Ervin showed that for going from ROH to F^-(HOR) (R = CH_3, CH_3CH_2, $(CH_3)_2CH$, $(CH_3)_3C$), only for R = CH_3 does the rotational barrier, calculated at the MP2/6-311 + G(2*df*,2*p*)// MP2/6-31G(*d*) level, decrease (from 1.1 to 0.3 kcal mol^{-1}) [60]. For the other three alcohol molecules, the rotational barriers increase around 0.9 kcal mol^{-1}. The main source for the decrease in the rotational barriers of the CH_3 and CF_3 groups are the increases of the C–O and C–F distances, respectively, upon complex formation of Cl^- and CH_3OCF_3. For $Cl^-((CH_3)_2O)$, no structure for the so-called staggered-eclipsed conformation was found, thus making determination of the CH_3 barrier in this complex impossible. Of course the binding in $Cl^-((CH_3)_2O)$ is completely different from $Cl^-(CH_3OCF_3)$. It does not seem unreasonable to assume that the barrier for CH_3 rotation in $Cl^-((CH_3)_2O)$ will be somewhat larger than in $(CH_3)_2O$. In $Cl^-((CF_2H)_2O)$ a large increase in the rotational barrier compared to $(CF_2H)_2O$ can be observed, from 1.0 to 7.5 kcal mol^{-1}, thus adding to the suggestion that the CF_2H rotations get locked in the chloride ion complex.

4.6. Natural population analysis charges

Natural population analysis (NPA) [51] charges calculated at the MP2/2//MP2/1 level of theory indicated that replacing hydrogen atoms by fluorine atoms hardly changes the NPA charges on the remaining hydrogen atom(s). In fact the NPA charge of the hydrogen atoms in $(CF_2H)_2O$ and CF_3OCF_2H are somewhat less positive than in $(CH_3)_2O$. For CF_3OCH_3 there is a small increase in the NPA charges on the three hydrogen atoms relative to $(CH_3)_2O$. The NPA charges in the chloride ion-(fluorinated) ether complexes were calculated at the MP2/[2/4]//MP2/[1/3] level of theory. In $Cl^-((CH_3)_2O)$ no charge transfer from Cl^- to the hydrogen atoms interacting with it is observed. In fact, the hydrogen atoms interacting with Cl^- will have a smaller NPA charge, while the axial hydrogen atoms will have a substantially larger NPA charge (from 0.15*e* to 0.20*e*). In the $Cl^-((CF_2H)_2O)$ and $Cl^-(CF_3OCF_2H)$ clusters more charge transfer from Cl^- can be observed. More interesting is the fact that a fairly large increase in the NPA of the hydrogen atom(s) interacting with Cl^- is observed. The smallest increase is, as expected, for $Cl^-(CH_3OCF_3)$, followed by $Cl^-((CF_2H)_2O)$ (rotamers 1 and 2 more than rotamer 4), and $Cl^-(CF_3OCF_2H)$. Hardly any changes in NPA charges are observed on the carbon, oxygen, and fluorine atoms upon complex formation with chloride ion.

5. Conclusions

The $\Delta H°$ and $\Delta S°$ values obtained by PHPMS for chloride ion clustering onto various (fluorinated) ethers

clearly show the influence of the fluorine substitution pattern on the thermochemistry. The experimental trends are confirmed by high level ab initio computations at the MP2/[2/4]//MP2/[1/3] levels of theory. Structures obtained at the MP2/[1/3] level of theory confirm expected binding characteristics, and show the existence of various stable rotamers and isomers. For the $Cl^-((CF_2H)_2O)$ cluster formation, a large negative $\Delta S°$ value was obtained that indicates locking of the two CF_2H groups in the complex relative to the free neutral. Standard methods in the quantum chemical software do not treat these features properly, and consequently a large discrepancy between $\Delta S°$ and $\Delta S°_{298}$ is observed. Good to excellent agreement is observed between $\Delta G°_{298}$ values from these PHPMS experiments and ICR experiments by Larson and McMahon. It was also shown that there is a driving force in $\Delta H°$ and not in $\Delta S°$, but the overall interaction of Cl^- with two hydrogen atoms will be more favorable than with one. Scaled normal mode vibrational frequencies calculated at the HF/6-31G(*d*) level of theory show good to excellent agreement with experimental values and computational data from B3LYP/6-311 ++ G(3*df*,3*pd*) computations. Finally for the $Cl^-(CH_3OCF_3)$ cluster it has been shown that at the MP2/[2/4]//MP2/[1/3] level of theory the rotational barrier for both the CH_3 and CF_3 groups will be lowered relative to free CH_3OCF_3. The observed changes are of course not unique to ethers. Similar experiments and computations were performed for chloride ion–(fluorinated) acetone clusters, and an even larger variation in thermochemistry and structure was observed [64].

Acknowledgements

The authors would like to thank the Natural Sciences and Engineering Research Council of Canada (NSERC) for continuing financial support. One of the authors (H.J.S.L.) thanks NSERC for an Undergraduate Student Research Award.

References

[1] W. Koch, W. L. Hase, Int. J. Mass Spectrom. 201 (2000) 1.
[2] G. Bouchoux, Y. Hoppilliard, J.-C. Tabet, Int. J. Mass Spectrom. 199 (2000) 1.
[3] M. T. Bowers, S. Graul, H. I. Kenttämaa, Int. J. Mass Spectrom. 195/196 (2000) 1.
[4] H. Schwarz, Int. J. Mass Spectrom. 185/186/187 (1999) 1.
[5] K. Takashima, J. M. Riveros, Mass Spectrom. Rev. 17 (1998) 409.
[6] S. M. Blair, J. S. Brodbelt, A. P. Marchand, K. A. Kumar, H.-S.Chong, Anal. Chem. 72 (2000) 2433, and references cited therein.
[7] M. More, D. Ray, P. D. Armentrout, J. Am. Chem. Soc. 121 (1999) 417, and references cited therein.
[8] S. E. Barlow, M. D. Tinkle, Rapid Commun. Mass Spectrom. 13 (1999) 390, and references cited therein.
[9] A. Mele, D. Pezzetta, A. Selvaa, Int. J. Mass Spectrom. 193 (1999) L1.
[10] K. B. Reiche, I. Starke, E. Kleinpeter, H.-J. Holdt, Rapid Commun. Mass Spectrom. 12 (1998) 1021, and references cited therein.
[11] D.V. Dearden, I.-H. Chu, J. Inclusion. Phenom. Mol. Recognit. Chem. 29 (1997) 269, and references cited therein.
[12] S.E. Hill, D. Feller, Int. J. Mass Spectrom. 201 (2000) 41, and references cited therein.
[13] A. Cattani, F.P. Schmidtchen, J. Prakt. Chem. 341 (1999) 291.
[14] M.M.G. Antoniss, B.M.H. Snellink-Ruël, I. Yigit, J.F.J. Engbersen, D.N. Reinhoudt, J. Org. Chem. 62 (1997) 9034.
[15] K. Tamao, T. Hayashi, Y. Ito, J. Organometal. Chem. 506 (1996) 85.
[16] J. Scheerder, J.F.J. Engbersen, A. Casnati, R. Ungaro, D.N. Reinhoudt, J. Org. Chem. 60 (1995) 6448.
[17] P.B. Savage, S.K. Holingren, S.H. Gellman, J. Am. Chem. Soc. 116 (1994) 4069.
[18] J. Scheerder, M. Fochi, J.F.J. Engbersen, D.N. Reinhoudt, J. Org. Chem. 59 (1994) 7815.
[19] D.E. Kaufman, A. Otten, Angew. Chem. 33 (1994) 1832.
[20] M.F. Hawtorne, X. Yang, Z. Zheng, Pure Appl. Chem. 66 (1994) 245.
[21] W.B. Farnham, D.C. Roe, D.A. Dixon, J.C. Calabrese, R.L. Harlow, J. Am. Chem. Soc. 112 (1990) 7707.
[22] M.E. Jung, H. Xia, Tetrahedron Lett. 29 (1988) 297.
[23] F.P. Schmidtchen, M. Berger, Chem. Rev. 97 (1997) 1609.
[24] J. Scheerder, J.F.J. Engbersen, D.N. Reinhoudt, Recl. Trav. Chim. Pays-Bas 115 (1996) 307.
[25] J.S. Brodbelt, S. Maleknia, C.-C. Liou, R. Lagow, J. Am. Chem. Soc. 113 (1991) 5913.
[26] J.S. Brodbelt, S. Maleknia, R. Lagow, T.Y. Lin, J. Chem. Soc. Chem. Commun. (1991) 1705.
[27] J.W. Larson, T.B. McMahon, J. Phys. Chem. 88 (1984) 1083.
[28] W. Zhang, Ch. Beglinger, J.A. Stone, J. Phys. Chem. 99 (1995) 11673.
[29] K. Norrman, T.B. McMahon, J. Am. Chem. Soc. 118 (1997) 2449.
[30] K. Norrman, T.B. McMahon, J. Phys. Chem. A 103 (1999) 7008.
[31] D.A. Good, M. Kamboures, R. Santiano, J.S. Francisco, J. Phys. Chem. A 103 (1999) 9230.
[32] D.A. Good, Y. Li, J.S. Francisco, Chem. Phys. Lett. 313 (1999) 267.
[33] D.A. Good, J.S. Francisco, J. Phys. Chem. A 103 (1999) 5011.

[34] L.K. Christensen, T.J. Wallington, A. Guschin, M.D. Hurley, J. Phys. Chem. A 103 (1999) 4202.
[35] D.A. Good, J.S. Francisco, J. Phys. Chem. A 102 (1998) 7143.
[36] D.A. Good, J.S. Francisco, J. Phys. Chem. A 102 (1998) 1854.
[37] V.B. Orgel, D.W. Ball, M.J. Zehe, J. Mol. Struct. (Theochem) 417 (1997) 195.
[38] R.A. Buono, R.J. Zauhar, C.A. Venanzi, J. Mol. Struct. (Theochem) 370 (1996) 97.
[39] K.-J. Hsu, W.B. DeMore, J. Phys. Chem. 99 (1995) 11141.
[40] A. Suga, Y. Mochizuki, N. Nagasaki, Y. Gotoh, H. Ito, S. Yamashita, T. Uchimaru, M. Sugie, A. Sekiya, S. Kondo, M. Aoyagi, Chem. Lett. (1994) 2365.
[41] Z. Zhang, R.D. Saini, M.J. Kurylo, R.E. Huie, J. Phys. Chem. 96 (1992) 9301.
[42] J.E. Szulejko, J.J. Fisher, T.B. McMahon, J. Wronka, Int. J. Mass Spectrom Ion Processes 83 (1988) 147.
[43] P. Kebarle, Techniques for the Study of Ion–Molecule Reactions (Techniques of Chemistry), W. Saunders, J.M. Farrer (Eds.), Wiley-Interscience, New York, 1988.
[44] M. Meot-Ner (Mautner), L.W. Sieck, Int. J. Mass Spectrom Ion Processes 109 (1991) 187.
[45] GAUSSIAN 98, Revision A.7, M.J. Frisch, G.W. Trucks, H.B. Schlegel, G.E. Scuseria, M.A. Robb, J.R. Cheeseman, V.G. Zakrzewski, J.A. Montgomery Jr., R.E. Stratmann, J.C. Burant, S. Dapprich, J.M. Millam, A.D. Daniels, K.N. Kudin, M.C. Strain, O. Farkas, J. Tomasi, V. Barone, M. Cossi, R. Cammi, B. Mennucci, C. Pomelli, C. Adamo, S. Clifford, J. Ochterski, G.A. Petersson, P.Y. Ayala, Q. Cui, K. Morokuma, D.K. Malick, A.D. Rabuck, K. Raghavachari, J.B. Foresman, J. Cioslowski, J.V. Ortiz, A.G. Baboul, B.B. Stefanov, G. Liu, A. Liashenko, P. Piskorz, I. Komaromi, R. Gomperts, R.L. Martin, D.J. Fox, T. Keith, M.A. Al-Laham, C.Y. Peng, A. Nanayakkara, C. Gonzalez, M. Challacombe, P.M.W. Gill, B. Johnson, W. Chen, M.W. Wong, J.L. Andres, C. Gonzalez, M. Head-Gordon, E.S. Replogle, J.A. Pople, Gaussian, Inc., Pittsburgh, PA, 1998.
[46] C.C.J. Roothan, Rev. Mod. Phys. 23 (1951) 69.
[47] C. Møller, M.S. Plesset, Phys. Rev. 46 (1934) 618.
[48] A.P. Scott, L. Radom, J. Phys. Chem. 100 (1996) 16502.
[49] A.E. Reed, R.B. Weinstock, F.J. Weinhold, J. Chem. Phys. 83 (1985) 735.
[50] A.L.L. East, L. Radom, J. Chem. Phys. 106 (1997) 6655.
[51] J.D.D. Martin, J.W. Hepburn, J. Chem. Phys. 109 (1998) 8139.
[52] L.A. Curtis, K. Raghavachari, P.C. Redferm, V. Rassolov, J.A. Pople, J. Chem. Phys. 109 (1998) 7764.
[53] G.D. Smith, R.L. Jaffe, H. Partridge, J. Phys. Chem. A 101 (1997) 1705.
[54] T.N. Gamble, M.Sc. Thesis, University of Waterloo, 2000.
[55] CRC Handbook of Chemistry and Physics, Ref. Data, 76th ed., D.L. Lide (Ed), CRC Press, Boca Raton, FL, 1995.
[56] C. Li, P. Ross, J.E. Szulejko, T.B. McMahon, J. Am. Chem. Soc. 118 (1996) 9360.
[57] H. Wang, G.H. Peslherbe, W.L. Hase, J. Am. Chem. Soc. 116 (1994) 9644.
[58] http://webbook.nist.gov./chemistry/ion.
[59] B. Bogdanov, M. Peschke, D.S. Tonner, J.E. Szulejko, T.B. McMahon, Int. J. Mass Spectrom. 185/186/187 (1999) 707.
[60] V.F. DeTuri, K.M. Ervin, J. Phys. Chem. A 103 (1999) 6911.
[61] B. Bogdanov, T.B. McMahon, J. Phys. Chem. A 104 (2000) 7871.
[62] P. Ayotte, J. Kim, J.A. Kelley, S.B. Nielsen, M.A. Johnson, J. Am Chem. Soc. 121 (1999) 6950.
[63] W.G. Fateley, F.A. Miller, Spectrochim. Acta 18 (1962) 977.
[64] B. Bogdanov, T.B. McMahon, unpublished.